



ELSEVIER

Contents lists available at ScienceDirect

Applied Radiation and Isotopes

journal homepage: www.elsevier.com/locate/apradiso

Chlorine signal attenuation in concrete

A.A. Naqvi^{a,*}, M. Maslehuddin^b, Khateeb ur-Rehman^a, O.S.B Al-Amoudi^c^a Department of Physics, King Fahd University of Petroleum and Minerals, Dhahran 31261, Saudi Arabia^b Center for Engineering Research, King Fahd University of Petroleum and Minerals, Dhahran 31261, Saudi Arabia^c Department of Civil & Environmental Engineering, King Fahd University of Petroleum and Minerals, Dhahran 31261, Saudi Arabia

HIGHLIGHTS

- Gamma ray yield measurements from chlorinated SF concrete at various depth.
- Cylindrical BGO detector.
- Portable neutron generator based PGNA setup.
- Nine 8 × 8 × 1 in³ SF cement concrete slabs and one chloride contaminated concrete slab.
- Monte Carlo Simulation to calculate 6.11 MeV gamma ray yield from various depth in SF cement concrete.

ARTICLE INFO

Article history:

Received 20 March 2015

Received in revised form

4 July 2015

Accepted 10 July 2015

Available online 11 July 2015

Keywords:

Chlorine gamma ray intensity measurement

silica fume cement concrete

Portable neutron generator based PGNA

setup

Monte Carlo simulations

ABSTRACT

The intensity of prompt gamma-ray was measured at various depths from chlorine-contaminated silica fume (SF) concrete slab concrete specimens using portable neutron generator-based prompt gamma-ray setup. The intensity of 6.11 MeV chloride gamma-rays was measured from the chloride contaminated slab at distance of 15.25, 20.25, 25.25, 30.25 and 35.25 cm from neutron target in a SF cement concrete slab specimens. Due to attenuation of thermal neutron flux and emitted gamma-ray intensity in SF cement concrete at various depths, the measured intensity of chlorine gamma-rays decreases non-linearly with increasing depth in concrete. A good agreement was noted between the experimental results and the results of Monte Carlo simulation. This study has provided useful experimental data for evaluating the chloride contamination in the SF concrete utilizing gamma-ray attenuation method.

© 2015 Elsevier Ltd. All rights reserved.

1. Introduction

The construction industry faces serious challenges due to corrosion of reinforcing steel, which is mainly caused by chloride ion contamination in concrete (ACI Committee 222, 1989; Al-Amoudi et al., 2001, 2002; Kirkpatrick et al., 2002; Maslehuddin et al., 1996; Poulsen and Mejlbro, 2006). It is highly desired to develop non-destructive techniques to assess chloride concentration in concrete to avoid damage due to reinforcement corrosion (Mohamed et al., (2008); Saleh and Livingston, 2000). Due to high capture cross section of thermal neutrons in chlorine, nuclear techniques, particularly Prompt Gamma Neutron Activation (PGNA), offer a prompt and reasonably accurate method to assess chlorine contamination in concrete. Recently, an accelerator based-PGNA setup has been developed successfully to determine

the chloride concentration in concrete (Naqvi et al., 2012, 2014). The portable neutron generator based PGNA setup developed by the authors in a previous study has been utilized to measure the intensity of chloride gamma-ray intensity emitted from various depths in silica fume (SF) cement concrete. The measured intensity of chloride gamma-ray emitted from chloride contaminants at a certain depth provide information about multiple factors, such as thermal neutron flux available at that depth as well as gamma-ray attenuation on the path to the detector. Such information is useful to generate chloride depth profile in concrete (Mohamed et al., (2008); Saleh and Livingston, 2000).

In the reported study, chloride measurements were carried out using a D–D reaction-based portable neutron generator-based PGNA setup to measure the intensity of chlorine gamma-ray at various depths of contaminated-chloride SF cement concrete specimen. Parallel to experimental studies Monte Carlo calculations were carried out to calculate the intensity of 6.11 MeV chlorine gamma-rays as a function of depth of the specimen for later comparison with the experimental data.

* Corresponding author.

E-mail address: anaqvi@kfupm.edu.sa (A.A. Naqvi).

2. Monte Carlo simulations for prompt gamma-ray yield calculations

Monte Carlo simulations were carried out to calculate the intensity of chlorine gamma-rays as a function of depth of the specimen. The geometry of the simulated PGNAA setup is shown in Fig. 1. The intensity of 6.11 MeV chlorine gamma-ray was measured from a rack containing nine concrete slabs each measuring 8 in × 8 in × 1 in stacked together using a portable neutron generator based PGNAA setup. The PGNAA setup used in this study is a modified form of the PGNAA setup described in other publications of the authors (Naqvi et al., 2012, 2014). The PGNAA setup utilized in the reported study mainly consists of a portable neutron generator, a cylindrical 25 cm × 8 cm (diameter × height) density polyethylene (HDPE) moderator and nine rectangular, 20 cm × 20 cm × 2.5 cm concrete slabs stacked together in a rack. The concrete slabs are placed on one side of the neutron generator (parallel to target-plane location), with the symmetry axis of the rack aligned at a right angle to neutron generator axis. The HDPE moderator disk is placed between the rack and the neutron generator with its symmetry axis aligned with the axis of the slabs rack. A cylindrical 12.5 cm × 12.5 cm (diameter × height) BGO gamma-ray detector views the concrete specimen at an angle of 45° with respect to its symmetry axis. In order to prevent undesired gamma-rays and neutrons from reaching the detector, lead, tungsten and paraffin neutron shielding are inserted between the neutron generator, moderator and the BGO detector, as shown in Fig. 1. The paraffin neutron shielding is made of a mixture of paraffin and lithium carbonate mixed in equal weight proportions.

Nine slab specimens were made of silica fume cement concrete by mixing 8 wt% SF and 92% ordinary Portland cement. Then one chlorinated contaminated SF cement concrete slab specimen was prepared by mixing 3% chloride ion, by weight of the cementitious material, following the procedure described elsewhere (Naqvi et al., 2012, 2014). Then, one of the uncontaminated SF cement concrete slab specimen was replaced by the contaminated SF cement concrete slab. Initially, the contaminated SF cement concrete slab was placed touching the moderator, at a distance of 1.25 cm between the moderator surface and the chlorinated SF concrete slab center. Fig. 1 shows PGNAA setup for a chloride contaminated slab placed at a distance of 11.25 cm from moderator surface (effective distance of 25.25 cm from neutron target). In the following discussion distance will be given from the center of chloride contaminated slab to the moderator surface. The moderator surface is fixed at a distance of 14 cm from the neutron target.

In the Monte Carlo studies, the distance of contaminated SF

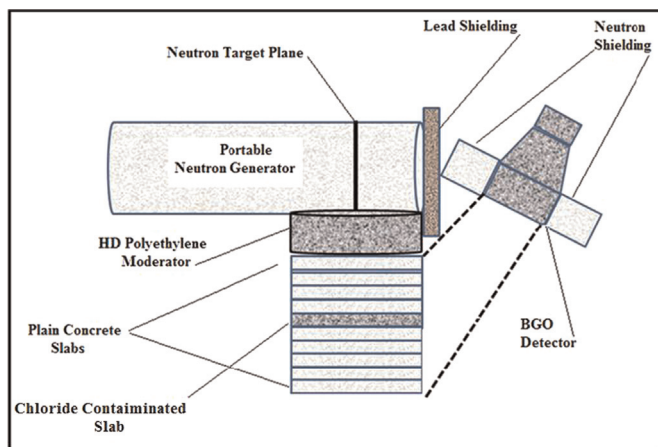


Fig. 1. Schematic of the MP320 portable neutron generator based PGNAA setup used to measure the prompt gamma-ray yield.

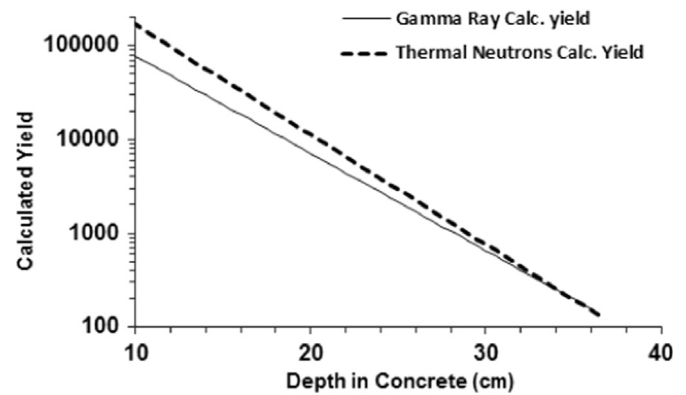


Fig. 2. Calculated thermal neutron intensity in a chloride-contaminated SF cement concrete slab at different distance (in cm) from the neutron source. Calculated yield of 6.11 MeV chlorine prompt gamma-rays from a chlorinated SF concrete slab located at different distance (in cm) in SF concrete slab from neutron target.

concrete slab was varied as 1.25, 6.25, 11.25, 16.25, and 21.25 cm from the moderator surface and the thermal neutron intensity was calculated at the contaminated slab location. Also, the intensity of 6.11 MeV chlorine gamma-rays detected in gamma-ray detector volume, was calculated for each distance of the slab from the moderator. These calculations were carried out using MCNP4B code (Briesmeister, 1997) running on a workstation utilizing dual AMD Athlon MP 2800+ processors. For simulation study, the moderators and sample cells were divided into sub-cells of 1 cm thickness. This allowed the study of the transport of the neutrons of appropriate statistical weight to the next adjacent cell, without any loss. F4 Tally was used to calculate the intensities of thermal neutrons and prompt gamma-rays. The calculation time varied from 12 h to 20 h for a statistical uncertainty of less than 3% in the results of the calculations.

The chemical composition of Portland cement, SF, and coarse and fine aggregate used in the simulations are listed in Table 1 (Maslehuiddin et al., 1996). The composition of Portland cement, SF, and coarse and fine aggregate were chosen as described earlier (Naqvi et al., 2005). Prompt gamma-rays with 6.11 MeV intensity were used to analyze the concentration of chlorine in the SF cement concrete specimen. Data on the prompt gamma-ray energies and intensities was taken from the work of (Choi et al., 2003). The bulk density of the sample was taken as 1.6 g/cm³. Notwithstanding the fact that the moisture content of dry concrete generally amounts to up to 1 wt%, due to its absorbency the moisture content in the specimens was assumed to be 5 wt%.

Fig. 2 shows the calculated thermal neutron intensity as a function of the depth of the concrete plotted on a semi-logarithmic scale. The calculated thermal neutron intensity $I(t)$ could be fitted as a function of thickness t using an exponential function fit of type $I(t) = c \exp(-at)$. For neutron calculated yield, the values of fit parameters were $c = 2.5 \times 10^6$ and $a = 0.270$ respectively along

Table 1
Chemical Composition (wt%) of Portland cement, silica fume, coarse and fine aggregates (Maslehuiddin, et al., 1996).

| Compound | Type I cement | Silica fume | Fine aggregate | Coarse aggregate |
|--------------------------------|---------------|-------------|----------------|------------------|
| SiO ₂ | 20.52 | 92.50 | 90.70 | 4.29 |
| Al ₂ O ₃ | 5.64 | 0.40 | 1.40 | 0.20 |
| Fe ₂ O ₃ | 3.80 | 0.40 | 0.48 | 0.23 |
| CaO | 64.35 | 0.50 | – | – |
| CaCO ₃ | – | – | 5.62 | 93.20 |
| MgO | 2.11 | 0.90 | 0.26 | 0.44 |
| SO ₃ | 2.1 | 0.50 | 0.2 | 0.4 |
| K ₂ O | 0.36 | 0.40 | 0.43 | 0.09 |
| Na ₂ O | 0.19 | 0.10 | 0.17 | 0.03 |

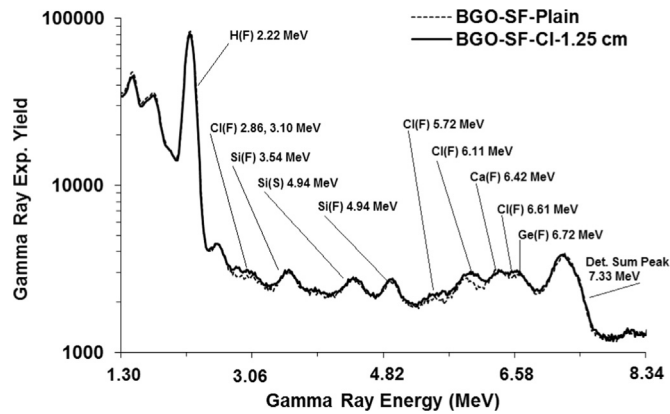


Fig. 3. Prompt gamma-rays spectra of chloride-contaminated SF cement concrete slab, at 1.25 cm from the moderator, superimposed upon uncontaminated SF concrete slabs gamma-ray spectrum over 1.30–8.34 MeV.

with a value of 99.7 for regression coefficient R^2 . The thermal neutron intensity decreases non-linearly with the depth. It is mainly due to $1/r^2$ dependence of the neutron flux at the slab location (where r is the distance from the neutron source to the contaminated SF slab). Additional contribution may come from increasing scattering and absorption of neutrons in concrete as the distance of the contaminated slab increases.

The calculated gamma ray yield data was also fitted with exponential fit similar to the neutron data fit. The values of fit parameters of gamma ray data were $c=0.85 \times 10^6$ and $a=0.239$ along with a corresponding value of 99.1 for regression coefficient R^2 . A decrease has also been observed in the calculated yield of 6.11 MeV chlorine prompt gamma-rays as a function of the distance from the neutron target. The prompt gamma-ray intensity decreases faster than the thermal neutron intensity because the neutron capture cross section is involved in 6.11 MeV prompt gamma-ray production. A further reduction in the prompt gamma-ray may be caused by decreasing solid angle of the neutron detector and increasing attenuation and multiple scattering of 6.11 MeV gamma-rays with increasing distance of the contaminated slab from the neutron target center.

3. Prompt gamma analysis of chlorinated SF cement concrete slabs

The intensity of 6.111 MeV chlorine gamma-ray was measured from concrete slabs rack containing nine uncontaminated concrete slabs each with 8 in \times 8 in \times 1 in dimension stacked together using a portable neutron generator based PGNAA setup. A pulsed beam of 2.5 MeV neutrons was produced via D(d,n) reaction using MP320 portable neutron generator. The neutron generator was operated with 70 keV deuteron beam with a pulse width of 5 ms and a frequency of 250 Hz. The pulsed neutron beam improves the signal to background ratio in the PGNAA studies. The typical beam current of the generator was 55–65 μ A. The thermal neutron spectra were acquired in PC-based data acquisition system utilizing multichannel buffer module Model 920E-16, ETHERNIM using a cylindrical 52 mm diameter and 2 mm thick enriched-Lithium glass thermal neutron detector, as described previously (Naqvi et al., 2012). The Li-glass was placed at 30° angle to neutron generator axis at a distance of 180 cm from the target plane location. The thermal neutron pulse height spectrum was recorded in 512 channels continuously during the experimental run and was integrated later on for thermal neutron flux normalization (Naqvi et al., 2012). Multichannel channel buffer model 'ORTEC Model 920E-16, ETHERNIM' is high performance multichannel

analyzer ideally suited for pulse height spectroscopy systems. The multichannel buffer was used with 'Scintivision' software of MAESTRO user interface package of ORTEC.

The prompt gamma-ray data from chloride-contaminated SF cement concrete slabs were acquired for 80–153 min. Shorter period for runs were utilized for the chloride-contaminated slab closer to the moderator.

4. Results and discussion

Fig. 3 shows prompt gamma-ray spectra, over 1.30–8.34 MeV, from SF cement concrete slabs with chloride-contaminated slab-center located at a distance of 1.25 cm from the moderator surface superimposed upon prompt gamma-ray spectra of SF plain concrete slabs without chloride contamination. The full energy peaks and single escape peaks are marked with letters (F) and (S), respectively. The hydrogen capture peak H(F) at 2.22 MeV is located on the left side of the spectrum while the large peak on the right end of the spectrum is the gamma-ray sum peak from activation of the BGO detector at 7.33 MeV, as was observed in the previous measurements (Naqvi et al., 2012, 2014). Prompt gamma-rays from chlorine interfering with those from SF cement concrete and BGO detector material, are located between the hydrogen capture peak and BGO detector activation sum peak. The chlorine prompt gamma-rays with energies in excess of 2.71 MeV were considered in study.

Fig. 4 shows enlarged view of Fig. 3 over 2.71–6.94 MeV. Due to poor energy resolution of the BGO detector, some of full energy and escape peaks of chlorine prompt gamma-rays are interfering with prompt gamma-rays from SF cement concrete and BGO detector material and could not be resolved. Fig. 4 shows resolved peaks of concrete constituents at Si(F) 3.54, Si(S) 4.94 MeV, Si(F) 4.94 and Ca(F) 4.42 MeV. Further, Fig. 4 shows interference between Cl(F) 6.61 MeV peak with Ca(F) 6.42 MeV peak as well as Ge(F) 6.72 MeV peaks. Similarly, the peaks of Cl(F) 5.72 MeV interfere with Cl(S) 6.11 MeV peaks. An unresolved broad chlorine prompt gamma-ray peak has been observed due to the interference of Cl(F) 2.86 and Cl(F) 3.10 MeV (Naqvi et al., 2012, 2014).

Figs. 5 and 6 are enlarged view of prompt gamma-ray spectra of SF cement concrete slabs with chloride-contaminated SF cement concrete block at 1.25, 6.25, 11.25, 16.25 and 21.25 cm from the moderator surface, superimposed upon each other. These

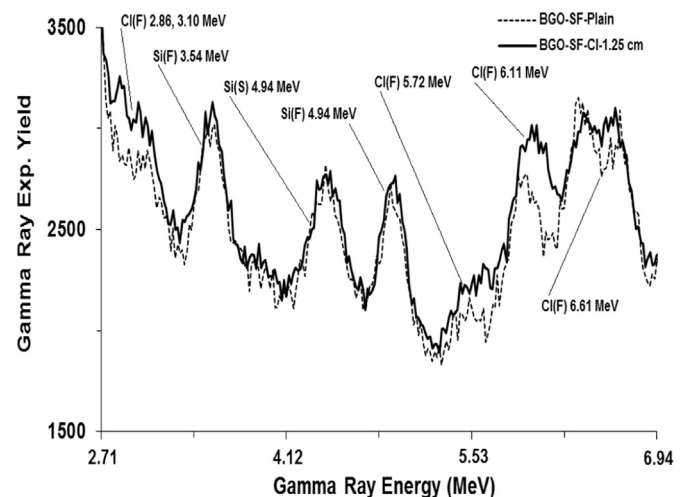


Fig. 4. Enlarged prompt gamma-rays spectra of chloride-contaminated cement concrete slab at 1.25 cm distance from the moderator superimposed upon the prompt gamma-ray spectrum of the uncontaminated SF cement concrete slabs over 2.71–8.34 MeV.

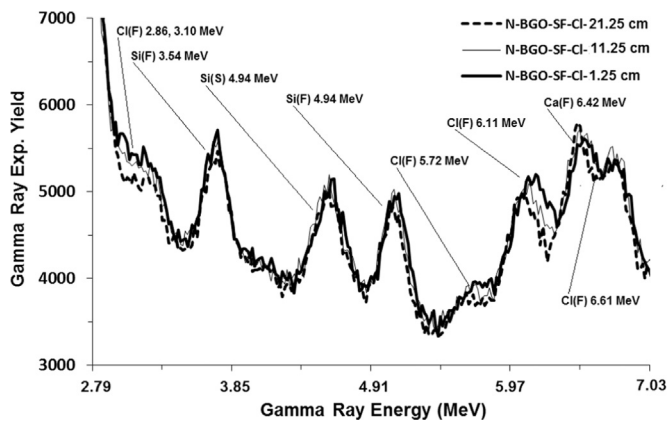


Fig. 5. Enlarged prompt gamma-rays spectra of chloride-contaminated cement concrete slab at 1.25, 11.25 and 21.25 cm distance from the moderator superimposed upon each other over 2.70–7.03 MeV.

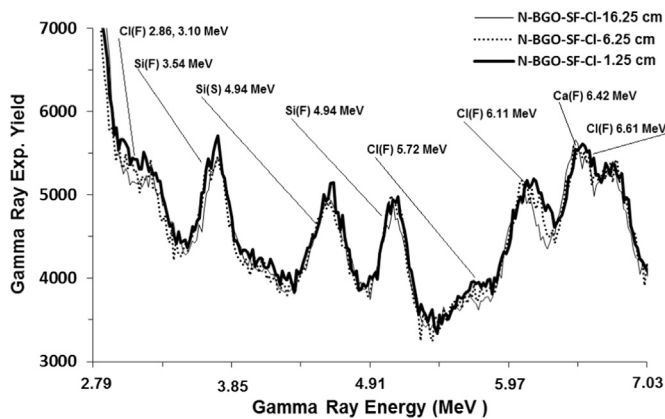


Fig. 6. Enlarged prompt gamma-ray spectra of chloride-contaminated cement concrete slab at 1.25, 6.25 and 16.25 cm distance from the moderator superimposed upon each other over 2.79–7.03 MeV.

correspond to 15.25, 20.25, 25.25, 30.25 and 35.25 cm from neutron target center, respectively. Well resolved Si(F) 3.54, Si(S) 4.94, Si(F) 4.94 and Ca(F) 4.42, Cl(F) 2.86 and Cl(F) 3.10 MeV gamma-ray peaks have been identified in Figs. 5 and 6. Also, interference between Cl(F) 5.72, Cl(F) 6.61 and Cl(F) 6.61 MeV with prompt gamma-rays from concrete constituents and detector material have been observed.

Both the figures show a decreasing trend of chlorine prompt gamma-ray yield as the distance of chloride contaminated slab increases from the moderator disk. This is due to decreasing thermal neutron flux at the location of chloride-contaminated slab with increasing distance from the moderator slab. The intensity of gamma-ray is further decreased due to increasing photon scattering with depth of the specimen.

Finally, the 6.11 MeV chlorine gamma-ray yield from the chloride-contaminated SF cement concrete slab spectra for 15.25, 20.25, 25.25, 30.25 and 35.25 cm distance was obtained after subtraction of prompt gamma-ray spectra of uncontaminated SF cement concrete specimen, described elsewhere in detail (Naqvi et al., 2012, 2014).

For each chloride concrete depth spectrum, corresponding net integrated count were obtained from the integration of corresponding difference spectrum. The difference spectrum was generated by subtracting plain SF concrete prompt gamma ray spectrum from the chloride depth spectrum. In the integrated yield error due to statistical uncertainties were included. No spectrum smoothing was done. Later integrated yield was compared with calculated yield obtained through Monte Carlo simulations.

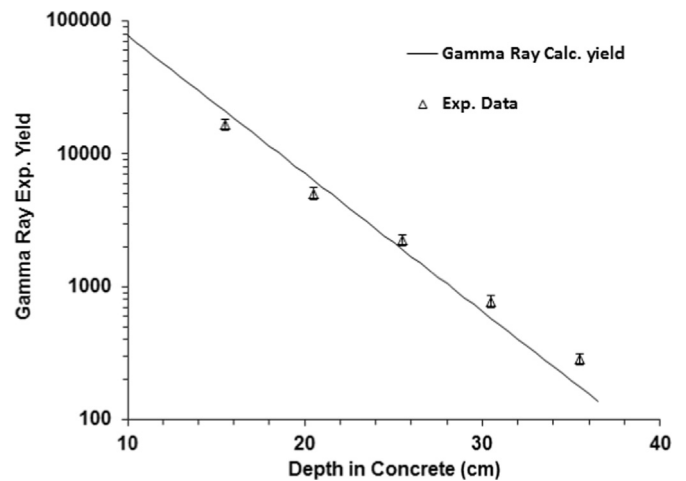


Fig. 7. Integrated yield of 6.11 MeV prompt gamma-ray spectra from contaminated SF cement concrete slabs at 1.25, 6.25, 11.25, 16.25, and 21.25 cm distance from moderator plotted as a function of effective distance from neutron target. Solid line represents the calculated yield obtained through Monte Carlo simulations.

Fig. 7 shows the integrated yield of 6.11 MeV as a function of effective depth (from neutron target center) of the chloride-contaminated SF concrete slabs. Also, superimposed upon the experimental data are calculated yield of 6.11 MeV chlorine prompt gamma-rays obtained through Monte Carlo simulations. There is good agreement between the experimental data and the calculated yield for concrete depth data at 15.25, 20.25, 25.25 and 30.25 cm but the data at 35.25 cm depth is slightly off as compared to calculated yield. This may be due to large uncertainty in reflected intensity of prompt gamma rays and also due to under-subtraction of background at that data point.

5. Conclusions

The intensity of prompt gamma-ray was measured from chloride-contaminated SF cement concrete specimens at various depth utilizing portable neutron generator based prompt gamma-ray setup. The intensity of 6.11 MeV chloride gamma-rays was measured from the chloride-contaminated slab at depths of 15.25, 20.25, 25.25, 30.25 and 35.25 cm. Due to attenuation of thermal neutron flux and emitted gamma-ray intensity the measured intensity of chlorine gamma-rays decreases non-linearly with increasing depth in concrete. There is agreement between the experimental results and the results of Monte Carlo simulation. This study has provided useful experimental data on chloride gamma-ray attenuation in SF cement concrete slabs for evaluating the chloride-contamination in the SF cement concrete.

Acknowledgments

This study is part of Project #RG1008 funded by the King Fahd University of Petroleum and Minerals (KFUPM), Dhahran, Saudi Arabia. The support provided by the Department of Physics and Center for Engineering Research, at KFUPM is also acknowledged.

References

- ACI Committee 222, 1989. Corrosion of Metals in Concrete. (ACI 222R-89), American Concrete Institute, Detroit, USA.
- Al-Amoudi, O.S.B., Maslehuddin, M., Bader, M.A., 2001. Characteristics of silica fume and its impact on concrete in the Arabian Gulf. *Concrete* 35 (2), 45–50.

- Al-Amoudi, O.S.B., 2002. Durability of plain and blended cements in marine environments. *Adv. Cem. Res.* 14 (3), 89–100.
- Briesmeister, J.F., 1997. MCNP4B2 A General Monte Carlo N-Particles Transport Code. Los Alamos National Laboratory Report, LA-12625-M. Version 4A.
- Choi, H.D., et al., 2003. Database of prompt gamma rays from slow neutron capture for elemental analysis, Nuclear Data Section, Division of Physical and Chemical Sciences, International Atomic Energy Agency (IAEA).
- Kirkpatrick, T.J., Weyers, R.E., Anderson-Cook, C.M., Sprinkel, M.M., 2002. Probabilistic model for the chloride-induced corrosion service life of bridge decks. *Cem. Concr. Res.* 32 (12), 1943–1960.
- Maslehuddin, M., Page, C.L., Rasheeduzzafar, 1996. *J. Mater. Civ. Eng.* 8, 63.
- Mohamed, A.B., Al-Sheikhly, M., Livingston, R.A., 2008. Monte Carlo simulations of a portable prompt gamma system for nondestructive determination of chloride in reinforced concrete. *Nucl. Instrum. Methods Phys. Res. B* 266, 3397–3405.
- Naqvi, A.A., Nagadi, M.M., Al-Amoudi, O.S.B., 2005. Measurement of lime/silica ratio in concrete using PGNA technique. *Nucl. Instrum. Methods Phys. Res. A* 554, 540–545.
- Naqvi, A.A., Kalakada, Zameer, Al-Matouq, Faris A., Nagadi, Maslehuddin, M., Al-Amoudi, O.S.B., ur-Rehman, Khateeb, 2012. Prompt gamma-ray analysis of chlorine in superpozz cement concrete. *Nucl. Instrum. Methods Phys. Res. A* 693, 67–73.
- Naqvi, A.A., Maslehuddin, M., Kalakada, Zameer, Al-Amoudi, O.S.B., 2014. Prompt gamma ray evaluation for chlorine analysis in blended cement concrete. *Appl. Radiat. Isot.* 94, 8–13.
- Poulsen, E., Mejlbro, L., 2006. *Diffusion of Chloride in Concrete: Theory and Application*. Taylor & Francis, London.
- Saleh, H.H., Livingston, R.A., 2000. Experimental evaluation of a portable neutron-based gamma spectroscopy system for chloride measurements in reinforced concrete. *J. Radioanal. Nucl. Chem.* 244 (2), 367–371.